



CHORUS

This is the accepted manuscript made available via CHORUS. The article has been published as:

Observation of multiple metastable states induced by electric pulses in the hysteresis temperature range of $1T\text{-TaS}_2$

Yongchang Ma, Zequn Wang, Yanhui Hou, Dong Wu, Cuimin Lu, and Cedomir Petrovic

Phys. Rev. B **99**, 045102 — Published 2 January 2019

DOI: [10.1103/PhysRevB.99.045102](https://doi.org/10.1103/PhysRevB.99.045102)

The observation of multi meta-stable states induced by electric pulses in the hysteresis temperature range of 1T-TaS₂

Yongchang Ma^{1,*}, Zequn Wang¹, Yanhui Hou¹,
Dong Wu², Cuimin Lu¹, and Cedimir Petrovic³

¹ *School of Materials Science and Engineering,
Tianjin University of Technology, Tianjin 300384, China*

² *International Center for Quantum Materials,
School of Physics, Peking University, Beijing 100871, China*

³ *Condensed Matter Physics and Materials Science Department,
Brookhaven National Laboratory, Upton, New York 11973, USA*

Abstract

The electric pulses induced responses of 1T-TaS₂ in the commensurate charge-density-wave phase in hysteresis temperature region (160~210 K) have been investigated. We observed an abrupt jump of the resistance excited by pulse, followed by a slow relaxation process in a time scale of ~100 s. At a fixed temperature, the various electric pulses can drive the system to multi meta-stable states. We propose that the spontaneous evolution or slow relaxation of the system by pulse excitations corresponds to the rearrangements of the textures of CCDW domains.

The strongly correlated electronic materials are the interesting systems for condensed matter scientists, as the carriers couple together and thus novel physical properties appear¹. The layered transition-metal dichalcogenides drive much attention in recent years, esp 1T-TaS₂: the observed ultra-fast resistance switching^{2,3}, the supercooled nearly commensurate charge-density-wave (CDW) phase at lower temperatures⁴, photosensitivity from visible to terahertz at room temperature⁵, and electrically driven reversible insulator-metal phase transition^{4,6}. Though the microscopic mechanisms have not been disclosed until now, it is believed that the associated transport properties are attributed to the novel electron structures.

1T-TaS₂ is one of the classical two-dimensional (2D) CDW systems. At room temperature, it reveals the nearly commensurate (NC) CDW. With decreasing temperature, a commensurate (C) CDW phase appears below 180 K whereas for heating process the CCDW state maintains up to 220 K, above which the NC phase establishes⁷⁻⁹. Scanning tunnelling microscopy has revealed that the NCCDW phase consists of trigonally packed CCDW domains separated by metallic regions that are not fully distorted⁹. As expected, the CCDW ground state is the starting point to understand the charge dynamics of the system^{4,10-13}. Besides the observations of hidden states and supercooled states at lower temperatures, the region 160 ~ 210 K is also interesting due to the remarkable hysteresis in dc transport properties, also known as the temperature region of metastability¹⁴. Photoemission spectroscopy, infrared conductivity and thermoelectric potential also exhibit hysteresis features¹⁵⁻¹⁷. Naively, understanding the properties in the hysteresis region would be inevitably related the CCDW and NCCDW phases.

Because of the close proximity of the various competing charge ordered phases in energy, several external perturbations or excitations can effectively modulated the CCDW phase^{2,4,18,19}, raising interesting questions about the dynamics near the phase transitions. Based on the accumulated results, the charge transport properties of 1T-TaS₂ are determined by sample dimensions, thermal history, photo excitation, electric field and pressure. These characteristics are believed to be supported by the intrinsic electrons and lattice structures, which range from microscopic processes of single carriers, through mesoscopic ordering of polarons, up to macroscopic frustrated structures^{3,12,20,21}.

The charged objects ranging from microscopic to macroscopic scales require that the responses in time domain should cover a wide range, therefore the time dependent responses

must be a useful probe for investigating the charge transport behavior, especially for the domains or domain walls^{9,22}. For a macroscopic sample, the NCCDW phase can not be supercooled and is not sensitive to medium electric fields at low temperatures^{3,4}, however, in the temperature region of metastability, the various activations may enable the transitions from a metastable state to other equilibrium state, and thus exhibiting more exotic properties. Further the potential applications for photon-electric devices or macroscopic sensors, also call for investigating the charge transport properties in bulk 1T-TaS₂ samples.

In this article, we systematically investigated the electric pulses induced responses of the CCDW phase of 1T-TaS₂ in the hysteresis temperature region. The pulses could drive the system to multi non-equilibrium states, exhibiting abrupt resistance jumps followed by slow relaxation processes exceeding several hundreds of seconds. To the best of our knowledge, the observed slow relaxations of the meta-stable states in the hysteresis temperature region, has not been reported yet.

The growth of 1T-TaS₂ single crystals could be found elsewhere²³. In the experiments, we focused on the in-plane transport properties of the sample with surface area $1.0 \times 0.2 \text{ mm}^2$ and thickness (along *c*-axis) about $20 \text{ }\mu\text{m}$, and the distance between the two potential electrodes is about 0.60 mm . After the sample was deposited on a polished sapphire, it was fixed mechanically and meanwhile connected electrically by silver paint. To check the validation of our experiments carried out in vacuum, two other approaches (the mounted sample, placed in nitrogen atmosphere or clamped mechanically between two sapphire substrates) were also applied, and the experimental results reproduced well. In CCDW state, the contact resistance is less than 1% of the bulk resistance, providing reliable measurement results. The experimental temperatures were monitored by a Cryo-con 32 controller with stability better than 0.01 K . To avoid Joule heating, a train of $50\text{-}\mu\text{s}$ electric pulses were applied to investigate the effects mainly from electric field.

The temperature dependent resistivity $\rho_{dc}(T)$, the CCDW transition temperature $T_{CCDW}=180 \text{ K}$, see Fig. 1(a), and the hysteresis feature upon warming are consistent with previous reports^{3,5,24}. In the following of context, the experimental data were obtained at fixed temperatures by warming the cryostat from a deep CCDW state below $T=120 \text{ K}$. The voltage or current data were recorded automatically by a computer. We will focus on the dc transport behavior of 1T-TaS₂ at fixed temperatures in the range $160 \sim 210 \text{ K}$.

Fig. 1(b) clearly shows the current voltage characteristic (CVC) of a typical 1T-TaS₂

sample, an abrupt jump appears when the electric field exceeding 10 V/cm (~ 600 mV). Similar results were reproduced well for other samples. Though these data were recorded by sweeping dc current, the Joule heating is negligible due to good thermal dissipation by the sapphire substrate²⁵; moreover, the resistance near zero current along the sweeping upon increasing current is distinctly different from the case of the inverse sweeping, corresponding to two different resistance states of the sample. We propose that this can not originate from the destruction of the sample under continuous dc current, as the subsequent measurements reproduced the previous data within experimental errors. The sweeping results definitely showed that the sample states are related to the history of the measurement. After several sweeping cycles, the resistance of the sample reaches an equilibrium, similar to the results reported by Yoshida *et al.*, though the samples dimensions and measurement temperatures are different⁴.

The transitions from one meta-stable state to another by current sweeping indicate that the electric field may have essential effects on the system. To disclose the evolution of the transport properties by dc current, we investigated the electric pulse response of 1T-TaS₂ samples systematically in the time domain. To avoid the Joule heating, the duration of pulses should be well shorter than τ_{SH} , the relaxation time of the sample by self-heating, $\tau_{SH} = \frac{N_M c}{\kappa} \cdot \frac{L}{S}$, where N_M is the number of moles of material with specific heat c and thermal conductance κ ²⁶, L and S are the length and the cross-section area of the specimen, respectively. In our experiments, $N_M \simeq 6.7 \times 10^{-8}$ mol, $c = 19.0$ J/(mol·K) at 200 K²⁷. For heat flow parallel to ab-plane, $\tau_{SH} \sim 27$ ms, whereas for the perpendicular direction, $\tau_{SH} \sim 80$ μ s^{28,29}. For an anisotropic system, the accurate calculation of the thermal relaxation time is difficult as the heat flows both directions at the same time. In experiments, for the pulses with duration less than 200 μ s, the undistorted wave form of the response indicates that the thermal effects could be neglected.

As shown in Fig. 1(c) after electric pulses, a jump appears indicating an abrupt decrease of the resistance, followed by a slow relaxation process, and then gradually saturates. With the decrease of temperature, as the CCDW condensation enhances, the less disturbance from the same electric field excitations and the magnitude of the resistance jumps decrease [Fig. 1(d)]. The sudden resistance jump may occur in a time scale of micro second or below, not related to heating effects. The inset of Fig. 2(a) shows typical oscilloscope traces of the voltage response of the sample to rectangular pulses, indicating a negligible thermal effects.

It is obvious that pulses change the configuration of the system to a new meta-stable state or that they tune one meta-stable state to another, possibly towards the minimum energy of the whole system. Further, the pulses subsequently applied again transfer the system state to other new ones. In our experiments, though we only used 5 voltage magnitudes at each temperature, it is believed that further applying pulses could also drive the system to distinct states with larger conductivities, till the NCCDW phase. In other words, there are multi meta stable states between CCDW and NCCDW phases, thus the energy differences between the meta-stable states would be very small. If it is the case, the thermal energy 200 K (17 meV) would smear out the distinctions between the multi meta-stable states^{16,31}, which is in conflict with the experimental data. Consequently, a reasonable mechanism is needed to explain the data, the multi meta-stable states induced by electric pulses³².

The Frenkel-Kontorova (FK) model of the incommensurate commensurate transition is a good selection to elucidate the behavior of the CDW systems. Vaskivskiyi *et al.* have used this model to analyze charge transport properties in hidden states of 1T-TaS₂ at lower temperatures. The model was originally devised to describe an array of atoms connected with harmonic springs, interacting with a periodic potential for a commensurate and incommensurate case in 1D case³³. Here we apply the FK model to the present system and the discrete responses of the resistance saturations observed in Figs. 1(d) and 2(a) correspond to discrete solutions of the Hamiltonian:

$$\mathcal{H} = \sum_n \left[\frac{1}{2a^2} \left(x_{n+1} - x_n - \frac{2\pi}{q_i} \right)^2 + V \left(1 - \cos \frac{2\pi x_n}{a} \right) \right] \quad (1)$$

where x_n are the positions of the n -th density wave maxima and a is the period of the underlying lattice.

It has been known that for Eq. 1, the periodicity $2\pi/q_i$ or wave vector q_i , changes as some parameters (temperature, pressure etc.) vary, forming the Devil's staircase³³. The numerous minima of the energy given by Eq. 1 form different meta-stable states of the system. A meta-stable state is expected to be a NCCDW-like phase with CCDW domains separated by metallic regions that are not fully distorted, where the conductance of the whole system varies with the ratio of the two components. Thus it is plausible that the multi equilibrium states in Figs. 1(c) and 1(d) correspond to different textures of the domains.

The data in Figs. 1(d) and 2(a) are reminiscent of the results of Vaskivskiyi *et al.*, in which the slow relaxations are clearly observed below 70 K³⁴. However, we emphasize

the very different temperature range. Moreover, we notice a distinction that there are no steps superposed on the relaxation curves in our results. As the magnitude of the pulse increases, the absolute jump increases and the expected resistance of the final equilibrium state decreases, though attempting to obtain its real value exceeding our endurance. We will discuss the reasons in the latter context.

The relaxation to a stable equilibrium state is well described by a stretched exponential model or by logarithmic time dependence^{34,35}. A possible mechanism is that the pinning centers prevent the wave numbers of the CDW's from reaching their equilibrium value after an electric pulse excitation and hence a non-equilibrium gap establishes. This viewpoint is from 1D CDW system, where the phase transitions from ICCDW to CCDW occurs³⁵. In the 2D NCCDW 1T-TaS₂ crystal, the system consists of trigonally packed CCDW domains and partly distorted metallic regions under electric pulses, thus may be adaptive to this framework. As the non-equilibrium gap is time dependent, the conductivity or the Ohmic resistance R of the specimen changes accordingly. Moreover, it is assumed that the relaxation to the equilibrium is induced by thermally activation. The relaxation rate γ depends on the temperature and on the local pinning strength h in the form $\gamma = (1/\tau_{ph})exp(-h/k_B T)$ where $1/\tau_{ph}$ is related to the phonon frequency.

For a wide distribution of the pinning strengths $P(h)$, the characteristic of the decay of metastable states is $I(t) = \int_0^\infty dh P(h)exp[-\gamma(h)t]$, which was originally applied for spin glasses by Ma³⁶. Such a decay is qualitatively similar with the analysis method in Refs.^{35,37}. We can quantify the decay times in pure 1T-TaS₂ by plotting a stretched exponential function (solid curves in Fig. 2) of the form $R(t) = R_0[1 - exp[-(t/\tau)^\beta]]$, with R_0 the measured equilibrium value after long time as expected, τ the characteristic time of the decay, β represents the distribution of the pinning energies, the larger β means the fast saturation towards a equilibrium state, indicating a large weight at lower energies of pinning strength³⁵. As shown in Fig. 2, for the electrical pulse of 15 V³⁰, neglecting the jump we obtain the parameters $\beta=0.36\pm 0.01$, $\tau=460$ s, fits well. The β is much less than the result in Ref.³⁷ where $\beta=1.50\pm 0.1$, obtained by the analysis of the two-time correlation function in the ICCDW state. However, due to the different temperature regions, the results from Refs.³⁵ and³⁷ may be corresponding to different physical mechanisms.

The slow relaxation process $\tau=460$ s, requests a large pinning strength h or a large energy barrier, $E_{BR} \simeq 6500$ K, if the phonon frequency is taken as 100 cm^{-1} and $k_B T \simeq 16.8$ meV. It

is a remarkably large value, compared with the thermal energy (~ 400 K) or the CCDW gap (~ 1100 K) from infrared spectrum¹⁶. According to the magnitude of the measured energy scale in Ref.²², the considerable energy barrier E_{BR} stands out and may be expected to act on individual domains, not associated with single particles. In other words, E_{BR} corresponds to the pinning energy per domain in 1T-TaS₂, though it is very difficult to characterize using conventional methods. Thus the following picture emerges for charge dynamics of 1T-TaS₂ in metastable temperature range: within the electric pulse duration, the CCDW phase is excited to bear a considerable strain or distortions and the NCCDW-like textures establish, absorbing or storing the extra energy from the external electric pulses, see Figs. 3 (a-b). After the electric pulse, to minimize or release excess energy of the system, an collective rearrangements of the CCDW domains from disturbed configurations to an ordered texture are requested, see Figs. 3 (c-d).

At a fixed temperature and under electric pulse of large magnitude, the CCDW phase and the resistance may be suppressed remarkably [Fig. 2(a)], and the equilibrium state may be corresponding to ordered smaller domains surrounded by the metallic regions with higher conductivities, as shown in Fig. 3(d). Hence it is believed that the larger change in conductivity by large electric pulses would mean stronger disorder of the domains, and consequently more time is necessary for the system to relax to an equilibrium state.

To demonstrate the connections between the observed resistance jump and the CCDW patterns, we propose a rough model to give an explanation. As shown in Fig. 4(a), the whole induced pattern has been transformed to a rectangle region for convenience, where the configuration of the CCDW domains are separated by metallic regions with low resistivity. The unit cells connect in series along the current direction, but in parallel perpendicularly. Obviously, the conductance of such a disordered state equals the re-arranged pattern in Fig. 4(b), in which the same cells have been aggregated. By adjusting the order of the rows in Fig. 4(b), the total resistance still keeps unchanged (Fig. 4(c), the CCDW component increases monotonically from top to bottom). Further, it is plausible that if the unit cells were taken much smaller, even a much more complex pattern could be approximated. For convenience, we focus on the case of a boundary of a straight line, as shown in Fig. 4(d).

To calculate the resistance in Fig. 4(d), the following parameters have been used: sample length \times width \times height(thickness)= $L \times W \times h$; the length of the transition region δ , A is the distance between the center of the transition region and the starting side, the total

resistance $R_T=R_{C\Box} + R_{M\Box} + R_{C\Delta}\parallel R_{M\Delta}$. It is obvious that $R_{C\Box}=\rho_C(A - \delta/2)/(W \cdot h)$, whereas $R_{M\Box}=\rho_M(L - A - \delta/2)/(W \cdot h)$, here ρ_C and ρ_M are the resistivity of the CCDW domains and the metallic regions, respectively. The last term $R_{C\Delta}\parallel R_{M\Delta}$ could be calculated by the integration method: the differentiate unit cell as indicated by dx connecting in parallel with each other:

$$\frac{1}{R_{C\Delta}\parallel R_{M\Delta}} = \int_0^W \frac{1}{\frac{\rho_C(\delta/W)x}{h \cdot dx} + \frac{\rho_M[\delta-(\delta/W)x]}{h \cdot dx}} \quad (2)$$

The integration term can be calculated out as $\frac{W \cdot h}{\rho_C \cdot \delta} \int_0^W \frac{dx}{x(1-\eta)+W \cdot \eta} = \frac{W \cdot h}{\rho_C \cdot \delta(1-\eta)} \ln \frac{1}{\eta}$, where $\eta = \frac{\rho_M}{\rho_C}$. Thus $R_T=\frac{\rho_C}{W \cdot h}[(A - \delta/2) + \eta(L - A - \delta/2) + \frac{\delta(\eta-1)}{\ln(\eta)}]$, indicating the resistance of the pattern is determined by both A and δ . As expected, the parameter A reflects the excitation effects of pulses and may correspond the total residual CCDW component, hence an abrupt decrease ($R_T/R_C < 1.0$) of the resistance exhibits (Fig. 5). After the end of the electric pulses, as the system gradually evolve towards a more stable state, the patterns may adjust themselves to an idealized order, $\delta \rightarrow 0$. This evolution corresponds to the vertical arrow line in Fig. 5, where δ decreases and therefore the resistance enhances gradually. In Fig. 5 the several thick crosses indicate the resistance of the eventually ordered states induced by electric pulses.

The slow relaxation process can be qualitatively explained by the generic Ostwald ripening model used for nucleation in crystal growth³⁸. In thermodynamically driven spontaneous process of a multiphase systems, large droplets grow at the expense of smaller ones to lower the overall energy. The droplets with size larger than R_c (critical radius) grow, while less than R_c shrink. To reduce the interfacial free energy of the system, the smaller droplets with high-curvature condense onto large, low-curvature droplets. For the present case, the energy gain comes from the fact that the energy per domain in the CCDW state is lower than the energy of an isolated one or a small cluster. It is likely that the main process may be the smaller domains merging into the existing larger ones, and in addition there would also include the shape readjustments of the clusters. Considering the time scale of the nucleation and growth process²⁰, the present clusters or domains would be much larger than a single David star. In very recent reports²¹, Frenzel *et al.* observed the smooth evolution from NC to C charge ordering over hundreds of CDW periods, indicating the existence of intermediate electronic phases with unique CDW order. To disclose weather the NCCDW components in such intermediate electronic phases are responsible for the charge dynamics observed in our

experiments is the following work.

In summary, the electric pulse induced responses of 1T-TaS₂ in the hysteresis temperature region has been investigated. At a fixed temperature, the pulses could drive the system to multi equilibrium states, exhibiting abrupt jumps followed by the slow processes exceeding several hundreds of seconds. We propose that the spontaneous decay or slow relaxation of the system by electric pulse corresponds to the rearrangements of the textures of CCDW domains.

ACKNOWLEDGMENTS: The research work was supported by the National Science Foundation of China (Grant No. 10704054). Work at Brookhaven National Laboratory is supported by the US DOE, Contract No. DE-SC0012704.

* Email: ycma@tjut.edu.cn

- ¹ Masatoshi Imada, Atsushi Fujimori and Yoshinori Tokura, *Rev. Mod. Phys.* **70**, 1039, (1998).
- ² L. Stojchevska, I. Vaskivskiy, T. Mertelj, P. Kusar, D. Svetin, S. Brazovskii, D. Mihailovic, *Science* **344**, 177 (2014).
- ³ I. Vaskivskiy, I. A. Mihailovic, S. Brazovskii, J. Gospodaric, T. Mertelj, D. Svetin, P. Sutar, and D. Mihailovic, *Nat. Commun.* **7**, 11442 (2016).
- ⁴ M. Yoshida, R. Suzuki, Y. J. Zhang, M. Nakano, and Y. Iwasa, *Sci. Adv.* **1**, e1500606 (2015).
- ⁵ D. Wu, Y. C. Ma, Y. Y. Niu, Q. M. Liu, Tao Dong, S. J. Zhang, J. S. Niu, H. B. Zhou, Jian Wei, Y. X. Wang, Z. R. Zhao, and N. L. Wang, *Sci. Adv.* **4**, eaao3057 (2018).
- ⁶ M. J. Hollander, Y. Liu, W. J. Lu, L. J. Li, Y. P. Sun, J. A. Robinson, and S. Datta, *Nano Lett.* **15**, 1861 (2015).
- ⁷ F. J. Di Salvo, J. A. Wilson, B. G. Bagley, and J. V. Waszczak, *Phys. Rev. B* **12**, 2220 (1975).
- ⁸ J. A. Wilson, F. J. Di Salvo, and S. Mahajan, *Adv. Phys.* **24**, 117 (1975).
- ⁹ R. E. Thomson, B. Burk, A. Zettl, John Clarke, *Phys. Rev. B.* **49**, 16899 (1994).
- ¹⁰ Ligu Ma, Cun Ye, Yijun Yu, Xiu Fang Lu, Xiaohai Niu, Sejoong Kim, Donglai Feng, David Tománek, Young-Woo Son, Xian Hui Chen and Yuanbo Zhang. *Nat. Commun.* **7**, 10956 (2016).
- ¹¹ D. Svetin, Igor Vaskivskiy, Serguei Brazovskii and Dragan Mihailovic, *Sci. Rep.* **7**, 46048 (2017).
- ¹² L. Perfetti, P. A. Loukakos, M. Lisowski, U. Bovensiepen, H. Berger, S. Biermann, P. S. Cornaglia, A. Georges, and M. Wolf, *Phys. Rev. Lett.* **97**, 067402 (2006).

- ¹³ Doohee Cho, Sangmo Cheon, Ki-Seok Kim, Sung-Hoon Lee, Yong-Heum Cho, Sang-Wook Cheong and Han Woong Yeom, *Nature Comm.* **7**, 10453 (2016).
- ¹⁴ A. W. Tsen, R. Hovden, D. Z. Wang, Y. D. Kim, J. Okamoto, K. A. Spoth, Y. Liu, W. J. Lu, Y. P. Sun, J. Hone, L. F. Kourkoutis, P. Kim, and A. N. Pasupathy, *Proc. Natl Acad. Sci. USA* **112**, 15054 (2015).
- ¹⁵ B. Dardel, M. Grioni, D. Malterre, P. Weibel, Y. Baer, and F. Levy, *Phys. Rev. B* **46**, 7407 (1992).
- ¹⁶ L. V. Gasparov, K. G. Brown, A. C. Wint, D. B. Tanner, H. Berger, G. Margaritondo, R. Gaál, and L. Forró, *Phys. Rev. B.* **66**, 094301 (2002).
- ¹⁷ T. Toshiro, O. Kenji, I. Takao and T. Shoji, *Physica* **105B**, 127 (1981).
- ¹⁸ B. Sipos, A. F. Kusmartseva, A. Akrap, H. Berger, L. Forro and E. Tuti *Nature Materials* **7**, 960 (2008).
- ¹⁹ Yijun Yu, Fangyuan Yang, Xiu Fang Lu, Ya Jun Yan, Yong-Heum Cho, Liguang Ma, Xiaohai Niu, Sejoong Kim, Young-Woo Son, Donglai Feng, Shiyang Li, Sang-Wook Cheong, Xian Hui Chen and Yuanbo Zhang, *Nature Nanotech.* **10**, 270 (2015).
- ²⁰ C. Laulhe, T. Huber, G. Lantz, A. Ferrer, S. O. Mariager, S. Grubel, J. Rittmann, J. A. Johnson, V. Esposito, A. Lubcke, L. Huber, M. Kubli, M. Savoini, V. L. R. Jacques, L. Cario, B. Corraze, E. Janod, G. Ingold, P. Beaud, S. L. Johnson, and S. Ravy, *Phys. Rev. Lett.* **118**, 247401 (2017).
- ²¹ Alex J. Frenzel, Alexander S. McLeod, Dennis Zi-Ren Wang, Yu Liu, Wenjian Lu, Guangxin Ni, Adam W. Tsen, Yuping Sun, Abhay N. Pasupathy, and D. N. Basov, *Phys. Rev. B* **97**, 035111 (2018).
- ²² G. Gruner, *Rev. Mod. Phys.* **60**, 1129 (1988).
- ²³ Yongchang Ma, Yanhui Hou, Cuimin Lu, Lijun Li and Cedomir Petrovic, *Phys. Rev. B* **97**, 195117 (2018).
- ²⁴ M. Yoshida, T. Gokuden, R. Suzuki, M. Nakano, and Y. Iwasa, *Phys. Rev. B* **95**, 121405(R) (2017).
- ²⁵ As the thermal conductivity κ along *c*-axis of 1T-TaS₂ is absent, the case of TiS₂ (a related compound, also space group $\bar{P}3m1$, 4.21 W/(m·K) at room temperature) has been used as a reference [H. Imai, Y. Shimakawa, and Y. Kubo, *Phys. Rev. B* **64**, 241104(R) (2001)]. In our measurements configuration, the heat flow along the *c*-axis gives a large contribution to remove

the Joule heating. In this direction, the cross section area $S=0.6\text{ mm}\times 0.2\text{ mm}$, to maintain a temperature difference of 1.0 K, the temperature gradient $\lambda=1.0\text{ K}/(20\mu\text{m}\times 0.5)=10^5\text{ K/m}$, the power needed should be no less than $P_1 = \kappa\lambda S = 36\text{ mW}$ at $T=200\text{ K}$, if $\kappa=3\text{ W}/(\text{m}\cdot\text{K})$. For the case of dc current 30 mA, the heating power is about $P_2 = I^2 R=(30\text{ mA})^2\times 20\text{ ohm}=18\text{ mW}$, indicating a temperature difference is less than 1.0 K. Nevertheless, in experiments, we measured the response signal for the pulse magnitude of 2.5 V, the thermally induced change of the resistance was about 4%. In the CVC data shown in Fig. 1b, the voltage is less than 0.65 V, hence the sample heating could be neglected within experimental errors.

- ²⁶ Marshall J. Cohen and A. J. Heeger, Phys. Rev. B **16**, 688 (1977).
- ²⁷ J. B. Balaguru Rayappan, S. A. Cecil Raj, N. Lawrence, Physica B **405**, 3172, (2010).
- ²⁸ In our experiments, the relaxation time of the sample is about several ms in the range of temperatures in the hysteretic region. The value $\tau_{SH} \sim 80\ \mu\text{s}$ is obtained if $\kappa=3\text{ W}/(\text{m}\cdot\text{K})$ along the c-axis.
- ²⁹ M. D. Nunnez-Regueiro, J. M. Lopez-Castillo, and C. Ayache, Phys. Rev. Lett. **55**, 1931 (1985).
- ³⁰ The magnitude of the electric pulses, as have been indicated in the inset of Fig. 1c, it is not associated to the sample alone, but the sum of the sample and R_L . The real potential magnitude through the sample during the pulse depends on the sample resistance.
- ³¹ Doohee Cho, Gyeongcheol Gye, Jinwon Lee, Sung-Hoon Lee, Lihai Wang, Sang-Wook Cheong and Han Woong Yeom, Nature Comm., **8**, 392 (2017).
- ³² Under an electric field the charge injection effects might also exist, as gate-controlled intercalation can induce the decreases of the resistance or even phases transition in 1T-TaS₂¹⁹, hence to separate the effects caused by the electric field from the effects induced by the charge injection, more investigations are necessary. However, this is not the focus of the present paper.
- ³³ P. Bak, Rep. Prog. Phys. **45**, 587 (1982).
- ³⁴ I. Vaskivskiy, J. Gospodaric, S. Brazovskii, D. Svetin, P. Sutar, E. Goreshnik, I. A. Mihailovic, T. Mertelj, D. Mihailovic, Sci. Adv. **1**, e1500168 (2015).
- ³⁵ G. Mihaly and L. Mihaly, Phys. Rev. Lett. **52**, 149 (1984).
- ³⁶ S. K. Ma, Phys. Rev. B **22**, 4484 (1980).
- ³⁷ Jun-Dar Su and Alec R. Sandy, Jyoti Mohanty, Oleg G. Shpyrko, Mark Sutton, Phys. Rev. B **86**, 205105 (2012).
- ³⁸ C. Sagui, D. S. OGorman, and M. Grant, Phys. Rev. E **56**, R21 (1997).

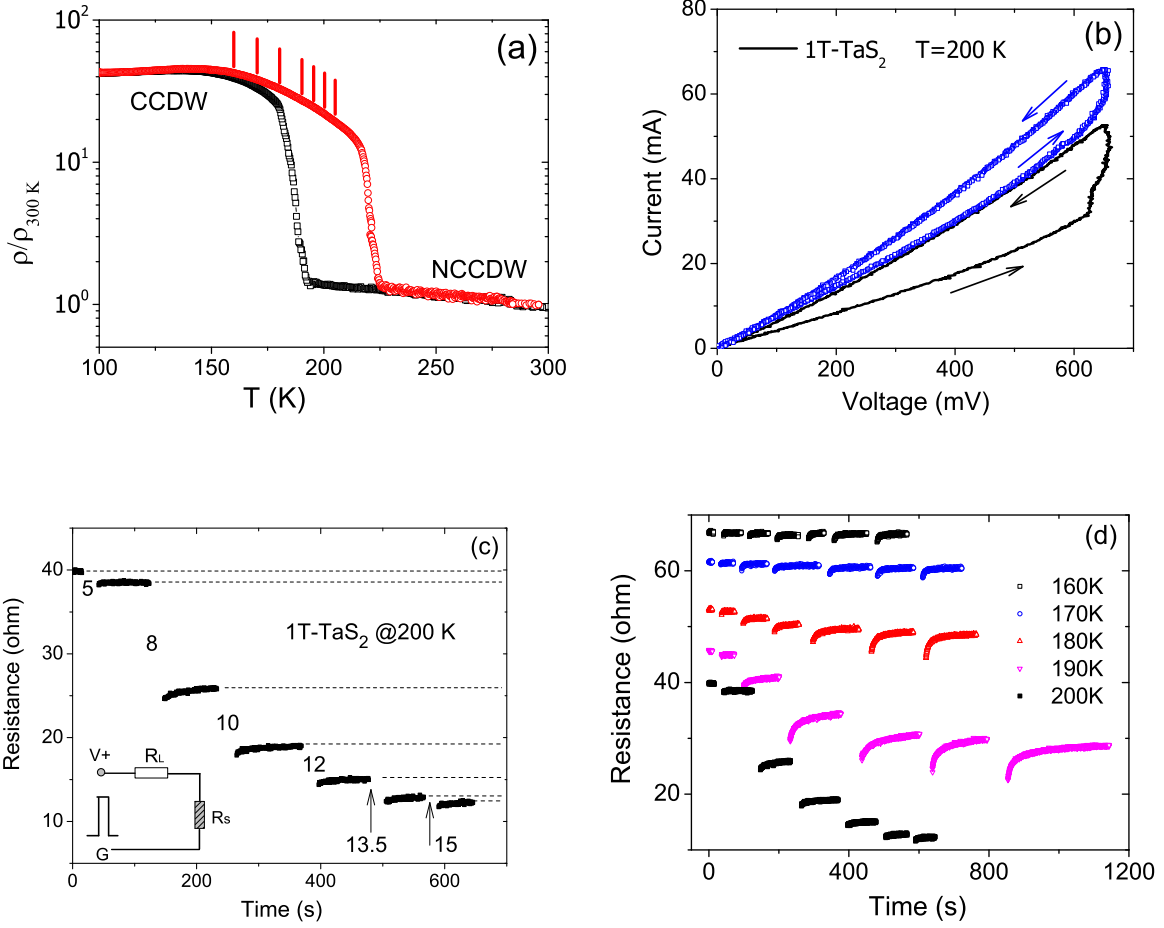


FIG. 1: (Color online) (a) The temperature dependent resistance (normalized to 300 K) in the ab-plane of 1T-TaS₂ crystal. The short lines in red color indicate the several fixed temperatures at which the responses excited by electrical pulses were measured. (b) The typical current voltage characteristics (by sweeping current) up to 650 mV of 1T-TaS₂ at 200 K. For clarity, only the data of two cycles are shown. (c) Time dependence of dc resistance R_S at $T=200\text{K}$, after the electric pulses³⁰. The inset is the schematic circuit of the measurement with a reference resistor $R_L=20\ \Omega$. After 5 s of the end of the pulse, the resistance is timely measured. (d) Similar to (c), at various temperatures.

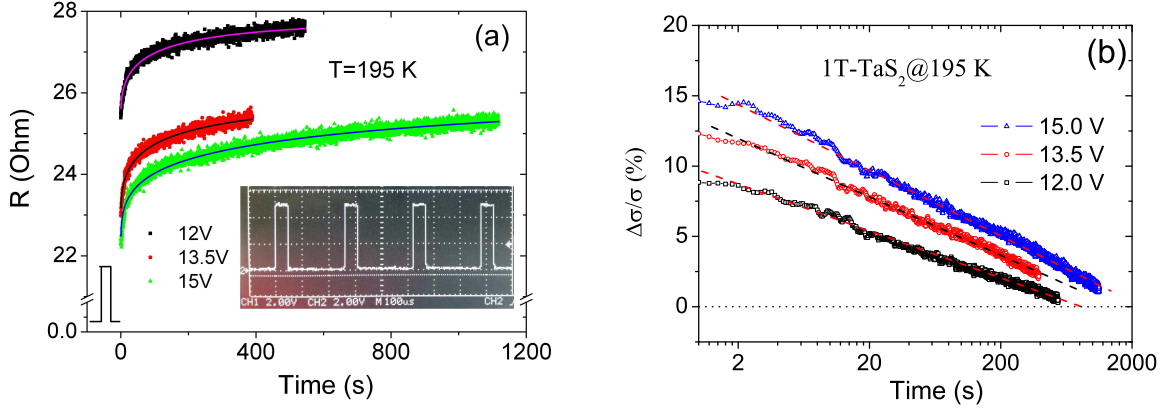


FIG. 2: (Color online) (a) Relaxation of the resistance R at 195 K after electric pulses³⁰. For each measurement, the sample was excited by electric pulses with duration 50- μ s to avoid Joule heating. The inset shows typical oscilloscope traces of the voltage response of the sample to rectangular pulses. Fits to $R(t)$ using a stretched exponential function. (b) Time dependence of $\Delta\sigma/\sigma_0$ after electric pulses at 195 K. The decrease as time elapses corresponds to the spontaneous decay of meta-stable states.

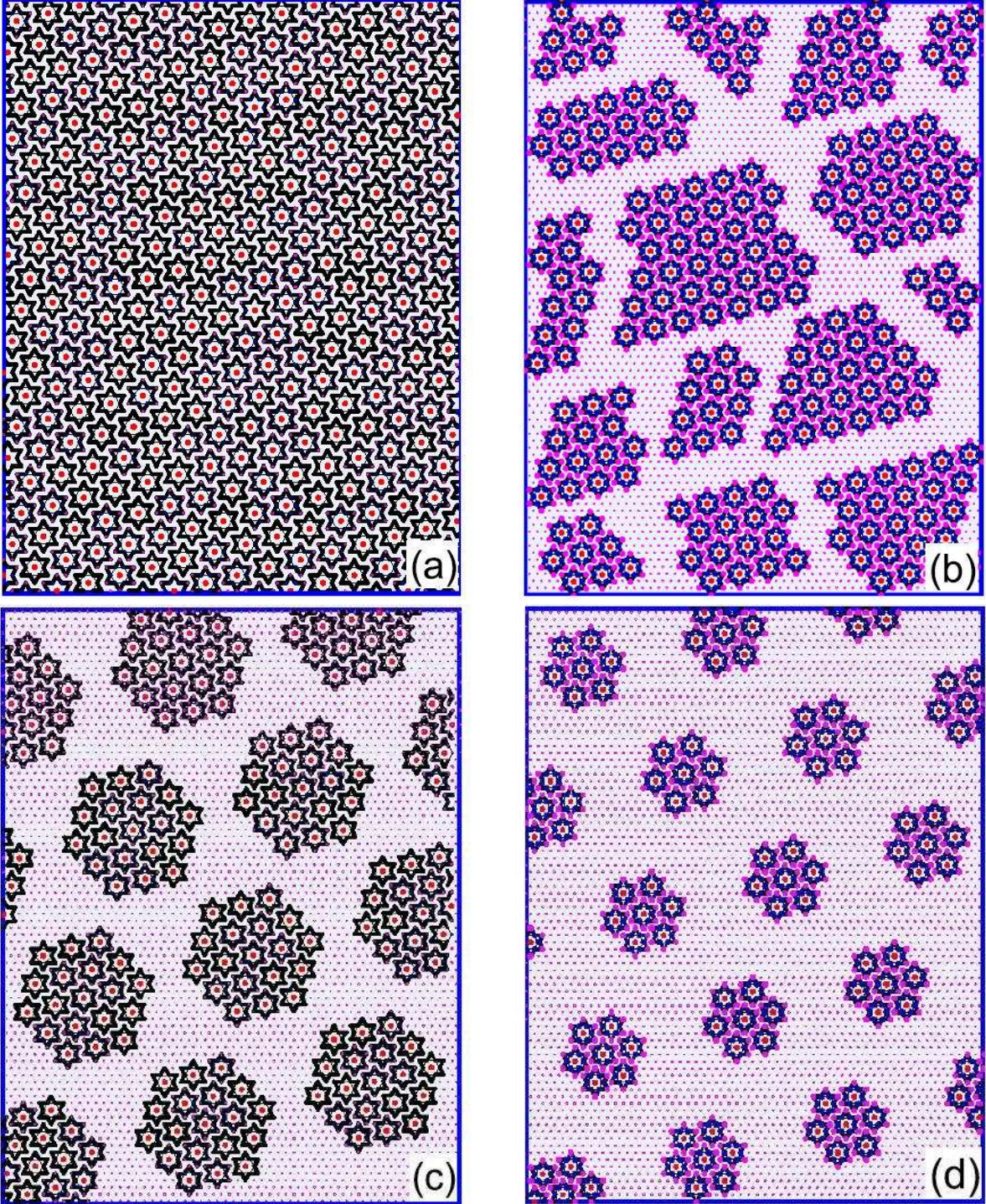


FIG. 3: (Color online) Real-space CDW reordering of electronic structure. (a) Idealized diagram of CCDW phase. (b) The schematic non-equilibrium pattern of the clusters after an electric pulse of 1T-TaS₂ in real space. (c) The schematic illustration for the charge arrangements at an equilibrium long time after an excitation of electric pulse. (d) Similar to (c) but by pulses with a larger magnitude.

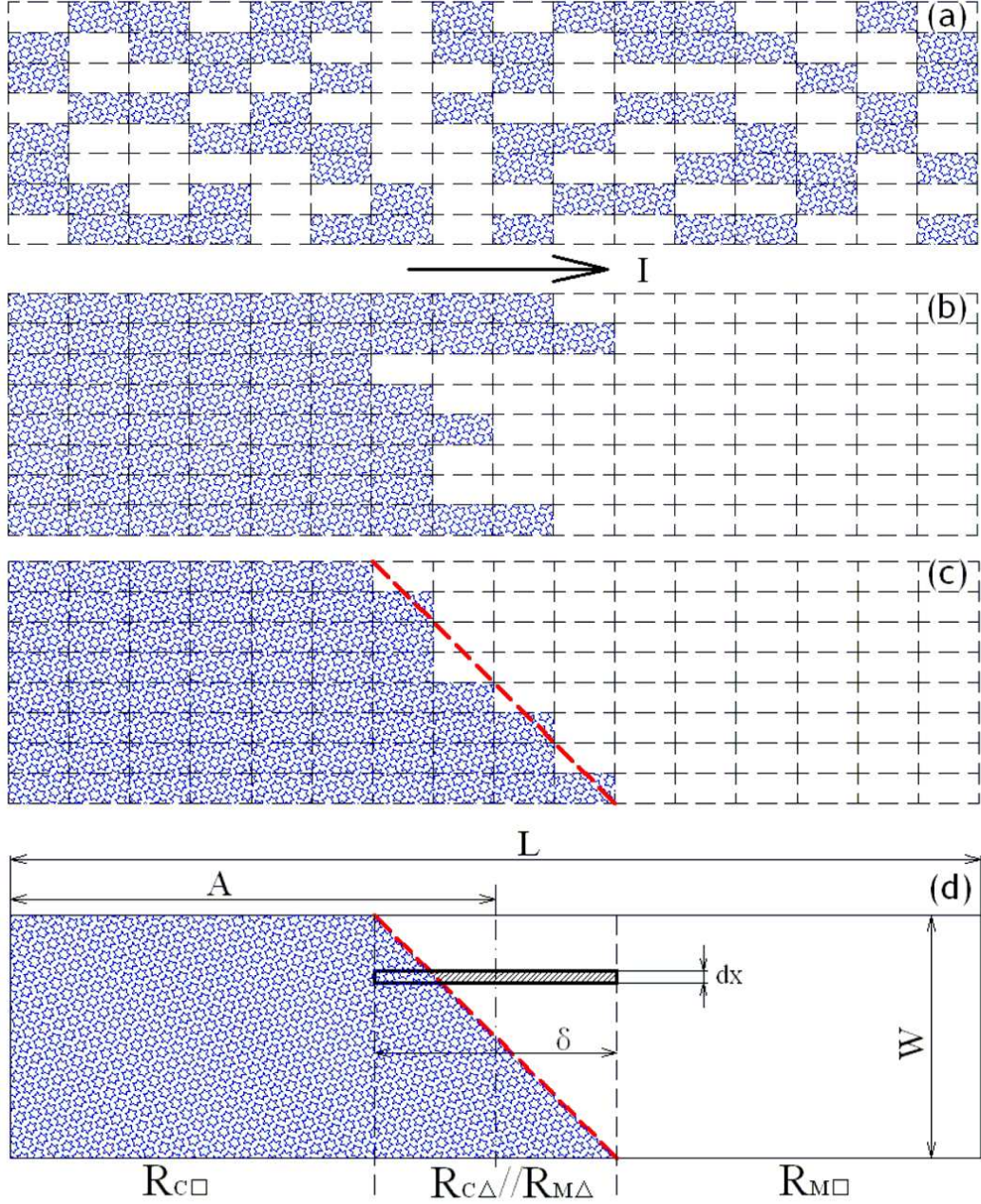


FIG. 4: (Color online) (a) The schematic non-equilibrium pattern of the clusters induced by electric pulses, the star regions denote the CCDW domains, whereas the others corresponds to the metallic regions with high conductivity. (b) The re-arranged pattern of (a), by aggregating the same textures in each row. (c) The further adjusted pattern of (b) without changing the total resistance. The dashed line only indicates an approximate boundary. (d) The schematic figure for calculating the total resistance, the dx indicates a differential unit. For convenience, we focus on the case of a straight boundary line.

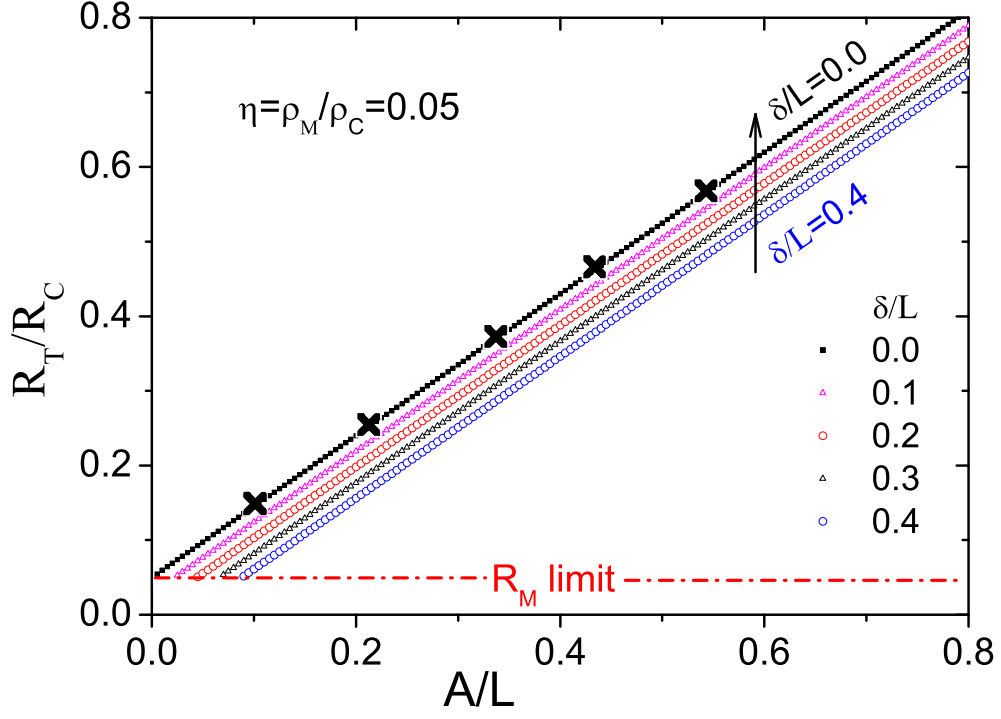


FIG. 5: The resistance of a typical pattern calculated using Eq. 2. R_C and R_M are the resistances of the pure CCDW and pure metallic states of the sample, respectively. The several thick crosses on the line with $\delta=0$ indicate the resistance values of the eventually ordered states.